Theor Chem Account (2008) 119:445–451
DOI 10.1007/s00214-007-0402-7

REGULAR ARTICLE

Theoretical studies on the reactions of acetone with chlorine atom and methyl radical

Hui Zhang · Gui-ling Zhang · Jing-yao Liu · Miao Sun · Bo Liu · Ze-sheng Li

Received: 11 October 2007 / Accepted: 28 November 2007 / Published online: 4 January 2008

Abstract Theoretical investigations are carried out on the reaction multi-channel $CH_3COCH_3 + Cl$ (R1) and $CH_3COCH_3 + CH_3$ (R2) by means of direct dynamics methods. The minimum energy path (MEP) is obtained at the MP2/6-31 + G(d,p) level, and energetic information is further refined at the BMC–CCSD (single-point) level. The rate constants are calculated by the improved canonical variational transition state theory (ICVT) with the small-curvature tunneling (SCT) correction in a wide temperature range 200–3,000 K. The theoretical overall rate constants are in good agreement with the available experimental data and are found to be $k_1 = 3.08 \times 10^{-17} T^{2.03} \exp(-32.96/T)$ and $k_2 = 1.61 \times 10^{-23} T^{3.53} \exp(-3969.51/T)$ $cm^3 molecule^{-1} s^{-1}$.

Keywords Gas-phase reaction · Transition state · Rate constants

Electronic supplementary material The online version of this article (doi:10.1007/s00214-007-0402-7) contains supplementary material, which is available to authorized users.

H. Zhang · G.-l. Zhang · M. Sun · B. Liu (✉)
College of Chemical and Environmental Engineering,
Harbin University of Science and Technology,
Harbin 150080, People's Republic of China
e-mail: liubo200400@vip.sina.com

H. Zhang
e-mail: hust_zhanghui1@hotmail.com

J.-y. Liu · Z.-s. Li
Institute of Theoretical Chemistry,
State Key Laboratory of Theoretical and Computational Chemistry,
Jilin University, Changchun 130023, People's Republic of China

1 Introduction

Acetone is an important representation of volatile organic compounds (VOCs), which are emitted from a variety of anthropogenic and natural sources into the atmosphere. In addition to these direct emissions, atmospheric oxidation of volatile hydrocarbons constitutes a significant source of various ketones. In the degradation of non-halogenated hydrocarbons, acetone is known to be long-lived (several months) [1]. The accumulation of acetone in the upper troposphere and lower stratosphere has recently been highlighted [2–4]. Acetone has been shown to be a potentially important source of HOx radicals (OH and HO_2), resulting in an increased ozone production and impacting on global ozone formation. The gas-phase reaction of Cl atoms with acetone is an important loss process for Cl atoms and acetones in the upper atmosphere. Hence, investigation on the accurate kinetic properties of the reactions for radicals with acetone is necessary in the atmospheric chemistry field.

In particular, in the past recent years many researches have been devoted to the kinetic studies of the reaction of acetone with the Cl atoms and methyl radical [5–18]. The reported values at room temperature for the rate constant of Cl with acetone were 3.06×10^{-12} (by Orlando et al. [5] and Notario et al. [6]), 2.2×10^{-12} (by Carr et al. [7], Martínes et al. [8], Wallington et al. [9], and Christensen et al. [10]), $(2.93 \pm 0.20) \times 10^{-12}$ (by Albaladejo et al. [11]), and $(1.69 \pm 0.32) \times 10^{-12}$ (by Olsson et al. [12]) (in units of $cm^3 molecule^{-1} s^{-1}$). The rate constants for the reaction between acetone and methyl radicals have been determined in literatures from 1950–1996 [14–17], the temperature range is from 300 up to 940 K.

To better understand the kinetics property of the two reactions, two alternative reaction channels a and b for each reaction have been investigated in this paper. The title reactions

can proceed through H-abstraction from the CH_3 groups and CH_3-abstraction from the acetone, i.e.,

$$Cl + CH_3COCH_3 \rightarrow CH_2COCH_3 + HCl \quad (R1a)$$
$$\rightarrow CH_3CO + CH_3Cl \quad (R1b)$$
$$CH_3 + CH_3COCH_3 \rightarrow CH_2COCH_3 + CH_4 \quad (R2a)$$
$$\rightarrow CH_3CO + C_2H_6 \quad (R2b)$$

Because the temperature used in the experiment is mostly at the lower end of the temperature range of practical interest, theoretical investigation is desirable to give a further understanding of the reaction mechanism of the two multiple channel reactions and to evaluate the rate constant at high temperatures. To our best knowledge, no previous theoretical work has addressed these reactions.

In order to obtain more reliable results for the rate constants and branching ratio in the title reactions over a wide temperature range 200–3,000 K, dual-level direct dynamics methods are employed in the present study. The potential energy surface information, including geometries, energies, gradients, and force constants of the stationary points (reactants, products, and transition states) and 16 extra points along the minimum energy path (MEP), is obtained directly from electronic structure calculations. Subsequently, by means of POLYRATE 9.1 program [18], the rate constants are calculated by using the variational transition state theory (VTST) proposed by Truhlar and co-workers [19,20]. The comparison between theoretical and experimental results is discussed.

2 Computational method

In the present work, the equilibrium geometries and frequencies of all the stationary points are optimized at the restricted or unrestricted second-order Møller–Plesset perturbation (MP2) [21–23] level with the 6-31 + G(d,p) basis set. Molecular electrostatic potentials [24] of CH_3COCH_3, Cl atom, and CH_3 radical are calculated at the same level, and plotted using gOpenMol 2.32 [25]. The MEP is obtained by intrinsic reaction coordinate (IRC) theory in mass-weighted Cartesian coordinates with a gradient step-size of 0.05 $(amu)^{1/2}$ bohr. At the same level, the energy derivatives, including gradients and Hessians at geometries along the MEP, are obtained to calculate the curvature of the reaction path and the generalized vibrational frequencies along the reaction path. Furthermore, the energy profile is refined by the BMC–CCSD method [26] [a new multi-coefficient correlation method based on the coupled cluster theory with single and double excitations (CCSD) proposed by Lynch and Truhlar] based on the MP2/6-31 + G(d,p) geometries. All electronic structure calculations are performed by means of GAUSSIAN03 program package [27].

The VTST [19,20] is employed to calculate the rate constants by the POLYRATE 9.1 program [18]. The improved canonical variational transition-state theory (ICVT) [28] with the small-curvature tunneling (SCT) [29,30] contributions proposed by Truhlar et al. [20,31] is applied to evaluate the theoretical rate constants. Most of the vibrational modes were treated as quantum-mechanical separable harmonic oscillators except for a few lower modes. The hindered-rotor approximation of Truhlar and Chuang [32,33] is used for calculating the partition function of these modes. In the calculation of the reactant electronic partition function, two electronic states of Cl atoms, $^2P_{1/2}$ and $^2P_{3/2}$, are included, with an 881 cm^{-1} splitting due to spin–orbit coupling. The curvature components are calculated using a quadratic fit to obtain the derivative of the gradient with respect to the reaction coordinate.

3 Results and discussions

3.1 Stationary points

The optimized geometric parameters of the reactants (CH_3COCH_3 and CH_3), products (CH_3COCH_2, HCl, CH_3CO, CH_3Cl, CH_4 and C_2H_6), and transition states (TS1a, TS1b, TS2a, and TS2b) for four reaction channels (R1a, R1b, R2a, and R2b) calculated at the MP2/6-31 + G(d,p) level are presented in Fig. 1, along with the available experimental data [34,35]. It can be seen that the theoretical geometric parameters of CH_3COCH_3, CH_3, CH_3Cl, C_2H_6, CH_4, and HCl are in good agreement with the corresponding experimental values [34,35]. For the transition states TS1a and TS1b, the lengths of C–H and C–C bond which will be broken stretch by 30 and 31% compared to the regular lengths of C–H and C–C bond in CH_3COCH_3, and the forming H–Cl and C–Cl bonds are elongated by about 12 and 21% over the equilibrium bond length in isolated HCl and CH_3Cl, respectively. On the other hand, in the structures of TS2a and TS2b, the C–H and C–C bonds, which will be broken, are stretched by 21 and 24% compared with the equilibrium bond lengths in isolated CH_3COCH_3, respectively; and the forming bonds C–H and C–C are elongated by 22 and 26% with respect to the equilibrium bond lengths of the molecules CH_4 and C_2H_6, respectively. These results imply that the barriers of reactions R1a and R1b are both near the corresponding products, and consequently, both of them will proceed via late transition states, while reactions R2a and R2b may proceed via a symmetrical barrier.

Table 1 lists the harmonic vibrational frequencies of all the stationary points involved the reactants, products, and transition states at the MP2/6-31 + G(d,p) level as well as the corresponding available experimental results [35]. The four transition states in Table 1 are confirmed by normal-mode

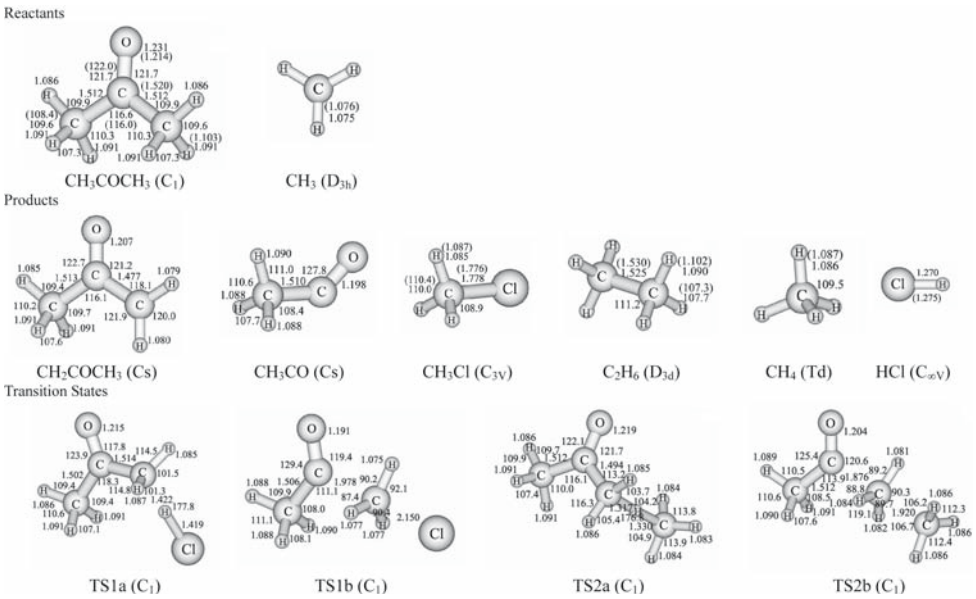

Fig. 1 Optimized geometries of the reactants, products, and transition states at the MP2/6-31 + G(d,p) level. The values in *brackets* are the experimental values ([34] for CH_3COCH_3, CH_3, CH_3Cl, CH_4, and C_2H_6, [35] for HCl). Bond lengths are in angstroms, and angles are in degrees

analysis to have only one imaginary frequency corresponding to the stretching modes of the coupling between breaking and forming bonds. The values of those imaginary frequencies are $1,093i$ cm^{-1} for reaction R1a, $847i$ cm^{-1} for reaction R1b, $1,835i$ cm^{-1} for reaction R2a, and $1,478i$ cm^{-1} for reaction R2b.

3.2 Energetics

The reaction enthalpies at 298 K (ΔH^0_{298}) and the potential barrier heights (ΔE^{TS}) with zero-point energy (ZPE) corrections for reactions R1a, R1b, R2a, and R2b calculated at the BMC–CCSD//MP2/6-31 + G(d,p) level are listed in Table 2, as well as the available experimental reaction enthalpies. The theoretical values at 298 K of ΔH^0_{298}, −7.0 kcal/mol for reaction R1a, 0.8 kcal/mol for reaction R1b, −7.4 kcal/mol for reaction R2a, and −5.6 kcal/mol for reaction R2b, are in good agreement with the corresponding experimental values, -7.4 ± 0.1, 0.8 ± 1.0, -8.8 ± 0.4, and -5.5 ± 0.9 kcal/mol, respectively, which were derived from the standard heats of formation (Cl, 28.97 kcal/mol [34]; CH_3COCH_3, -52.19 ± 0.14 kcal/mol [35]; CH_2COCH_3, −8.61 kcal/mol [35]; HCl, −22.05 kcal/mol [34]; C_2H_6, -20.02 ± 0.07 kcal/mol [35]; CH_3, 34.80 kcal/mol [35]; CH_3CO, -2.87 ± 0.72 kcal/mol [35]; CH_3Cl, −19.99 kcal/mol [35]; CH_4, -17.53 ± 0.26 kcal/mol [35]).

A schematic potential energy surface of the title reactions obtained at the BMC–CCSD//MP2/6-31 + G(d,p) + ZPE level is described in Fig. 2. For reaction acetone with Cl atom, the barrier of TS1a taking the value of 0.88 kcal/mol at the BMC–CCSD//MP2 level is about 23.2 kcal/mol lower than that of TS1b, which indicates that H-abstraction channel from the CH_3 group is more favorable than the CH_3-abstraction channel from the CH_3COCH_3. At the same time, reaction R1a is more exothermic than reaction R1b by about 8.2 kcal/mol. On the basis of above calculation, reaction R1a is more favorable than reaction R1b both thermodynamically and kinetically and will dominate the reaction, while the CH_3-abstraction channel may be negligible. Similarly, for reaction acetone with CH_3 radical, the potential barrier heights are 11.9 kcal/mol for reaction R2a and 45.9 kcal/mol for reaction R2b at BMC–CCSD//MP2/6-31 + G(d,p) + ZPE level, and reaction channel R2a is more exothermic than R2b by about 2.2 kcal/mol. So reaction channel R2a is also more favorable than reaction channel R2b both thermodynamically and kinetically. H-abstraction channel (R2a) is expected to be the major one with larger rate constants, and the CH_3-abstraction channel is a minor pathway.

3.3 Rate constants

Theoretical calculations of the Cl + CH_3COCH_3 and CH_3 + CH_3COCH_3 reactions are carried out at the BMC–CCSD//MP2/6-31 + G(d,p) level. The rate constants of the individual channel, k_{1a} for R1a, k_{1b} for R1b, k_{2a} for R2a, and k_{2b} for R2b, are evaluated by conventional transition state theory (TST) and the improved canonical variational transition state theory (ICVT) in a wide temperature range from 200 to 3,000 K. Tunneling effect is included by means of the small-curvature tunneling (SCT) correction. The calculated TST, ICVT, and ICVT/SCT rate constants of the four reaction channels are given in Table S1 as supplementary information, and also plotted against the reciprocal of temperature in Fig. 3. It is shown that for reaction R1a, the TST, ICVT and ICVT/SCT rate constants are nearly the same in the whole temperature region, which indicates that both the variational effect and tunneling effect are almost negligible. It can also be seen that the ICVT and TST rate constants of the other

Table 1 Calculated and experimental frequencies (cm^{-1}) for the reactants, products, and transition states for the title reaction at the MP2/6-31+G(d,p) level

Species	MP2/6-31 + G(d,p)	Experimental
CH_3COCH_3	3255, 3254, 3208, 3203, 3121, 3117, 1762, 1529, 1518, 1510, 1509, 1435, 1430, 1278, 1139, 1108, 925, 909, 815, 536, 488, 384, 125, 48	3019[a], 2972, 2963, 2937, 1731, 1454, 1435, 1426, 1410, 1364, 1216, 1091, 1066, 891, 877, 777, 530, 484, 385
CH_3	3430, 3430, 3232, 1478, 1478, 469	3171[a], 3004, 1403
CH_2COCH_3	3392, 3270, 3256, 3125, 3125, 2094, 1516, 1514, 1502, 1430, 1292, 1098, 1056, 918, 832, 638, 538, 521, 388, 230, 81	
HCl	3112	2991[a]
CH_3Cl	3278, 3278, 3161, 1525, 1525, 1458, 1074, 1074, 781	3039[a], 2937, 1452, 1355, 1017, 732
CH_3CO	3242, 3236, 3122, 1939, 1506, 1505, 1406, 1083, 981, 899, 471, 74	1875[a], 1420
CH_4	3265, 3265, 3265, 3120, 1600, 1600, 1395, 1395, 1395	3019[a], 2917, 1534, 1306
C_2H_6	3224, 3224, 3203, 3203, 3124, 3123, 1549, 1549, 1547, 1547, 1477, 1449, 1259, 1259, 1043, 841, 841, 332	2985[a], 2969, 2954, 2896, 1469, 1468, 1388, 1379, 1190, 995, 822, 289
TS1a	3310, 3264, 3216, 3195, 3126, 2334, 1516, 1507, 1464, 1437, 1279, 1196, 1142, 1035, 974, 892, 872, 808, 571, 512, 482, 399, 333, 143, 103, 42, 1093*i*	
TS1b	3420, 3397, 3255, 3238, 3201, 3129, 2021, 1508, 1501, 1436, 1426, 1411, 1182, 1153, 1134, 1064, 1004, 909, 509, 458, 342, 238, 159, 130, 100, 73, 847*i*	
TS2a	3322, 3318, 3299, 3259, 3206, 3191, 3160, 3118, 2199, 1518, 1512, 1496, 1492, 1487, 1426, 1408, 1397, 1286, 1229, 1133, 1108, 994, 948, 834, 756, 641, 547, 514, 484, 386, 368, 118, 97, 42, 23, 1835*i*	
TS2b	3328, 3305, 3287, 3283, 3240, 3218, 3133, 3117, 3099, 2009, 1509, 1505, 1503, 1501, 1405, 1397, 1394, 1273, 1251, 1197, 1154, 1031, 987, 911, 767, 760, 544, 474, 384, 265, 252, 149, 148, 97, 54, 1478*i*	

[a] Ref. [35]

Table 2 The reaction enthalpies at 298 K (ΔH^0_{298}), the barrier heights TSs (ΔE^{TS}) (kcal/mol) with zero-point energy (ZPE) correction for the reactions of CH_3COCH_3 with Cl atom and CH_3 radical at the BMC–CCSD//MP2/6-31 + G(d,p) level together with the experimental value

		BMC–CCSD //MP2	Experimental
ΔH^0_{298}	$Cl + CH_3COCH_3 \rightarrow CH_2COCH_3 + HCl$ (R1a)	−7.0	-7.4 ± 0.1
	$Cl + CH_3COCH_3 \rightarrow CH_3CO + CH_3Cl$ (R1b)	0.8	0.8 ± 1.0
	$CH_3 + CH_3COCH_3 \rightarrow CH_2COCH_3 + CH_4$ (R2a)	−7.4	-8.8 ± 0.4
	$CH_3 + CH_3COCH_3 \rightarrow CH_3CO + C_2H_6$ (R2b)	−5.6	-5.5 ± 0.9
ΔE^{TS} + ZPE	$Cl + CH_3COCH_3 \rightarrow CH_2COCH_3 + HCl$ (R1a)	0.9	
	$Cl + CH_3COCH_3 \rightarrow CH_3CO + CH_3Cl$ (R1b)	24.1	
	$CH_3 + CH_3COCH_3 \rightarrow CH_2COCH_3 + CH_4$ (R2a)	11.9	
	$CH_3 + CH_3COCH_3 \rightarrow CH_3CO + C_2H_6$ (R2b)	45.9	

Experimental value derived from the standard heats of formation: Cl, 28.97 kcal/mol [34]; CH_3COCH_3, -52.19 ± 0.14 kcal/mol [35]; CH_2COCH_3, −8.61 kcal/mol [35]; HCl, −22.05 kcal/mol [34]; C_2H_6, -20.02 ± 0.07 kcal/mol [35]; CH_3, 34.80 kcal/mol [35]; CH_3CO, -2.87 ± 0.72 kcal/mol [35]; CH_3Cl, −19.99 kcal/mol [35]; CH_4, -17.53 ± 0.26 kcal/mol [35]

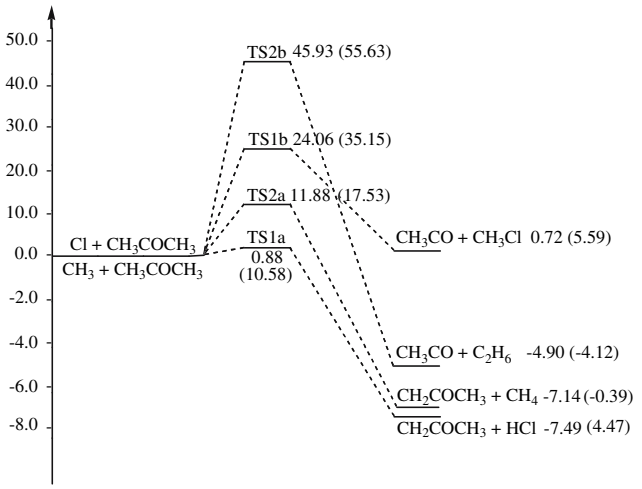

Fig. 2 Schematic potential energy surface for $Cl + CH_3COCH_3$ and $CH_3 + CH_3COCH_3$ reactions. Relative energies (in unit of kcal/mol) are calculated at the BMC–CCSD//MP2/6-31 + G(d,p) + ZPE level and the MP2/6-31 + G(d,p) + ZPE level (the values in *parentheses*)

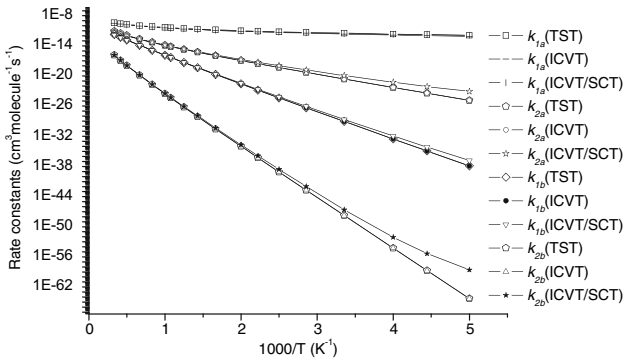

Fig. 3 The TST, ICVT and ICVT/SCT rate constants ($cm^3 molecule^{-1} s^{-1}$) calculated at the BMC–CCSD//MP2/6-31 + G(d,p) level for four reaction channels, k_{1a} for R1a, k_{1b} for R1b, k_{2a} for R2a, k_{2b} for R2b, versus 1,000/T between 200 and 3,000 K

three reaction channels are nearly the same in the whole temperature region, which indicates that the variational effect is almost negligible. And the tunneling effect of the other three reaction channels, i.e., the ratio between ICVT/SCT and ICVT rate constants, plays an important role at the lower temperatures and is negligible at high temperatures. For example, the ratios of k(ICVT/SCT)/k(ICVT) are 1.26×10, 6.22×10, and 4.94×10^5 at 200 K for R1b, R2a, and R2b, respectively, while they are 1.21, 1.44, and 1.63 at 600 K, respectively.

Figure 3 shows that the rate constants of reactions R1a, k_{1a}, are about 2–24 orders of magnitude higher than those of reaction R1b, k_{2b}, from 200 to 3,000 K. And the rate constants of reactions R2a, k_{2a}, are about 4–35 orders of magnitude higher than those of reaction R2b, k_{2b}, from 200 to 3,000 K. It can be concluded that the H-abstraction channel from the CH_3 group is always absolutely dominant in the temperature

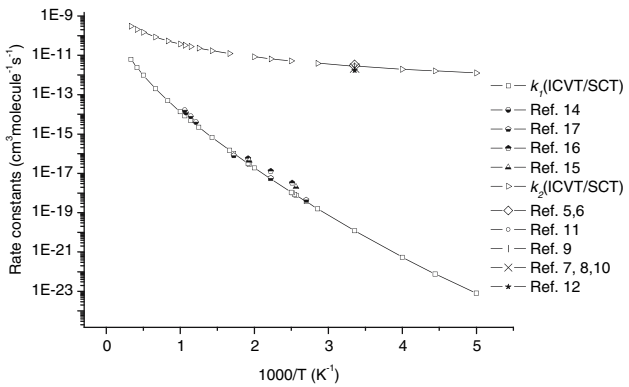

Fig. 4 The ICVT/SCT rate constants calculated at the BMC–CCSD//MP2/6-31 + G(d,p) level for $Cl + CH_3COCH_3$ and $CH_3 + CH_3COCH_3$ reactions k_1 and k_2 ($cm^3 molecule^{-1} s^{-1}$) versus 1,000/T between 200 and 3,000 K, together with the experimental value

range 200–3,000 K, and the CH_3-abstraction channel from the CH_3COCH_3 is a minor pathway on the corresponding reaction. This is consistent with a qualitative assessment based on the potential energy barrier heights and the reaction enthalpies of these reaction channels.

The overall theoretical ICVT/SCT rate constants k_1 and k_2 for the title reaction are calculated from the sum of the corresponding individual rate constants, i.e., $k_1 = k_{1a} + k_{1b}$, $k_2 = k_{2a} + k_{2b}$, which are displayed in Fig. 4 along with the corresponding experimental data [5–12,14–17]. The ICVT/SCT rate constants of k_1 at 298 K, 2.79×10^{-12} cm^3 $molecule^{-1} s^{-1}$, is in good agreement with the available experimental value [5–12], and the ratio of $k_{ICVT/SCT}/k$exptl remains within a factor of approximately 0.91–1.27. The ICVT/SCT rate constants of k_2 are in good agreement with the corresponding experimental values [14–17], the deviation between the theoretical and experimental values remains within a factor of approximately 0.30–1.27. The calculated activation energy is 14.14 kcal/mol, it is in good agreement with the corresponding experimental value 12.18 kcal/mol given by Hosein et al. [14]. Thus, the present calculations may provide reliable estimations of the rate constants for the $Cl + CH_3COCH_3$ and $CH_3 + CH_3COCH_3$ reactions over a wide temperature range.

For convenience of future experimental measurements, three-parameter fits of the ICVT/SCT rate constants of four reaction channels and the overall rate constants in the temperature range 200–3,000 K are performed and the expressions are given as follows (in unit of $cm^3 molecule^{-1} s^{-1}$):

$$k_1(T) = 3.08 \times 10^{-17} T^{2.03} \exp(-32.96/T)$$
$$k_2(T) = 1.61 \times 10^{-23} T^{3.53} \exp(-3969.51/T)$$

The molecular electrostatic potential is an important tool to analyze molecular reactivity because it can provide the information about local polarity. Figure 5 gives the distribution of the molecular electrostatic potential. There, the most

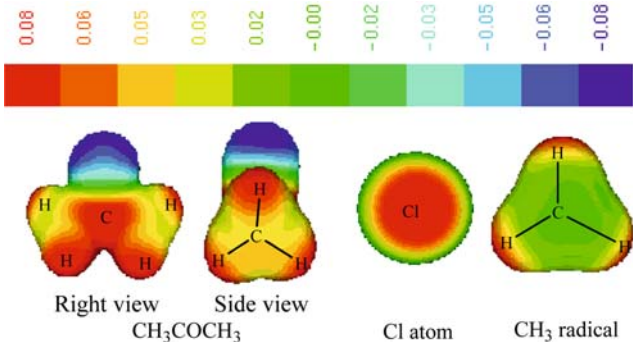

Fig. 5 The calculated electrostatic potential textured vDW surfaces for the reactants

negative and positive potentials are assigned to be blue and red, respectively, and the color spectrum is mapped to all other values by linear interpolation. The more positive potential bond (more red) will be more favored for the nucleophiles to attack at. It is found that in molecule CH_3COCH_3 the H atoms bear stronger positive potential (red) than the C atoms of CH_3 groups (yellow), indicating that the H atoms can be more easily attacked by the nucleophiles, i.e., the H-abstraction reaction channels will be expected much faster than the CH_3-abstraction reaction channels. Note that the Cl atom is encircled by marked negative potential, while the periphery of the CH_3 radical is mainly dominated by positive potential of the H atoms. Therefore, the Cl atom is more preferably to attack the H atom of CH_3COCH_3 comparing to the CH_3 radical. From these results we could confer that the reaction of $Cl + CH_3COCH_3$ could occur more easily than the $CH_3 + CH_3COCH_3$ reaction. This is in line with the rate constant results calculated above.

4 Conclusions

In this paper, the reactions $Cl + CH_3COCH_3$ and $CH_3 + CH_3COCH_3$ have been studied theoretically. The potential energy surface information is obtained at the MP2/6-31+G (d,p) level, and higher-level energies for the stationary points and a few extra point along the minimum energy path are further refined by the BMC–CCSD method. Two reaction channels are identified, one for H-abstraction from the CH_3 group, and the other for CH_3-abstraction from the CH_3COCH_3 for the two reactions. The calculated potential barriers show that major pathway is H-abstraction from the CH_3 group channel. For each individual reaction channel, the theoretical rate constants are calculated by the improved canonical variational transition state theory (ICVT) incorporating the small-curvature tunneling (SCT) contributions in the temperature range 200–3,000 K. The overall rate constants are in good agreement with the available experimental values. Owing to the good agreement between the theoretical and experimental values, the theoretical results should be useful for estimating the kinetics of the title reactions over a wide temperature range where no experimental data are available.

Acknowledgments The authors thank Professor Donald G. Truhlar for providing POLYRATE 9.1 program. This work is supported by the National Natural Science Foundation of China (20333050, 20303007 and 20272011), the Doctor Foundation by the Ministry of Education, the Foundation for University Key Teacher by the Department of Education of Heilongjiang Province (1151G019, 1152G010), the Key subject of Science and Technology by the Ministry of Education of China, the Key subject of Science and Technology by Jilin Province, and Natural Science Foundation of Heilongjiang Province (TA2005-15, B200605).

References

1. Singh HB, O'Hara D, Herlth D, Sachse W, Blake DR, Bradshaw JD, Kanakidou M, Crutzen PJ (1994) J Geophys Res 99:1805
2. Singh HB, Kanakidou M, Crutzen PJ, Jacob DJ (1995) Nature 378:50
3. Arnold F, Knop G, Zierens H (1986) Nature 321:505
4. Arnold F, Burger V, Drost-Fanke B, Grimm F, Schneider J, Krieger A, Stile T (1997) Geophys Res Lett 24:3017
5. Orlando JJ, Tyndall GS, Vereecken L, Peeters J (2000) J Phys Chem A 104:11578
6. Notario A, Mellouki A, Bras GL (2000) Int J Chem Kinet 32:62
7. Carr S, Shallcross DE, Canosa-Mas CE, Wenger JC, Sidebottom HW, Treacy JJ, Wayne RP (2003) Phys Chem Chem Phys 5:3874
8. Martínes E, Aranda A, Díaz-de-mera Y, Rodríguez A, Rodríguez D, Notario A (2004) J Atmos Chem 48:283
9. Wallington TJ, Andino JM, Ball JC, Japar SM (1990) J Atmos Chem 10:301
10. Christensen LK, Ball JC, Wallington TJ (2000) J Phys Chem A 104:345
11. Albaladejo J, Notario A, Cuevas CA, Ballesteros B, Martínez E (2003) J Atmos Chem 45:35
12. Olsson B, Hallquist M, Ljungström E, Davidsson J (1997) Int J Chem Kinet 29:195
13. Wallington TJ, Guschin A, Hurley MD (1998) Int J Chem Kinet 30:309
14. Mousavipour SH, Pacey PD (1996) J Phys Chem 100:3573
15. Arthur NL, Newitt PJ (1979) Aust J Chem 32:3486
16. Arican H, Arthur NL (1983) Aust J Chem 36:2185
17. Kinsman AC, Roscoe JM (1994) Int J Chem Kinet 26:191
18. Corchado JC, Chuang Y-Y, Fast PL, Villa J, Hu W-P, Liu Y-P, Lynch GC, Nguyen KA, Jackels CF, Melissas VS, Lynch BJ, Rossi I, Coitino EL, Ramos AF, Pu J, Albu TV (2002) POLYRATE version 9.1. Department of Chemistry and Supercomputer Institute. University of Minnesota, Minneapolis
19. Truhlar DG, Garrett BC (1980) Acc Chem Res 13:440
20. Truhlar DG, Isaacson AD, Garrett BC (1985) In: Baer M (ed) The theory of chemical reaction dynamics, vol 4, CRC press, Boca Raton, p 65
21. Duncan WT, Truong TN (1995) J Chem Phys 103:9642
22. Frisch MJ, Head-Gordon M, Pople JA (1990) Chem Phys Lett 166:275
23. Head-Gordon M, Pople JA, Frisch MJ (1988) Chem Phys Lett 153:503
24. Boris B, Petia B (1999) J Phys Chem A 103:6793
25. Bergman DL, Laaksonen L, Laaksonen A (1997) J Mol Graph Model 15:301
26. Lynch BJ, Zhao Y, Truhlar DG (2005) J Phys Chem A 109:1643

27. Frisch MJ, Trucks GW, Schlegel HB, Scuseria GE, Robb MA, Cheeseman JR, Montgomery JA, Jr, Vreven T, Kudin KN, Burant JC, Millam JM, Iyengar SS, Tomasi J, Barone V, Mennucci B, Cossi M, Scalmani G, Rega N, Petersson GA, Nakatsuji H, Hada M, Ehara M, Toyota K, Fukuda R, Hasegawa J, Ishida M, Nakajima T, Honda Y, Kitao O, Nakai H, Klene M, Li X, Knox JE, Hratchian HP, Cross JB, Adamo C, Jaramillo J, Gomperts R, Stratmann RE, Yazyev O, Austin AJ, Cammi R, Pomelli C, Ochterski JW, Ayala PY, Morokuma K, Voth GA, Salvador P, Dannenberg JJ, Zakrzewski VG, Dapprich S, Daniels AD, Strain MC, Farkas O, Malick DK, Rabuck AD, Raghavachari K, Foresman JB, Ortiz JV, Cui Q, Baboul AG, Clifford S, Cioslowski J, Stefanov BB, Liu G, Liashenko A, Piskorz P, Komaromi I, Martin RL, Fox DJ, Keith T, Al-Laham MA, Peng CY, Nanayakkara A, Challacombe M, Gill PMW, Johnson B, Chen W, Wong MW, Gonzalez C, Pople JA (2003) Gaussian 03. Gaussian, Inc., Pittsburgh
28. Garrett BC, Truhlar DG, Grev RS, Magnuson AW (1980) J Phys Chem 84:1730
29. Lu DH, Truong TN, Melissas VS, Lynch GC, Liu YP, Grarrett BC, Steckler R, Issacson AD, Rai SN, Hancock GC, Lauderdale JG, Joseph T, Truhlar DG (1992) Comput Phys Commun 71:235
30. Liu Y-P, Lynch GC, Truong TN, Lu D-H, Truhlar DG, Garrett BC (1993) J Am Chem Soc 115:2408
31. Steckler R, Hu W-P, Liu Y-P, Lynch GC, Garrett BC, Isaacson BAD, Melissas VS, Lu D-P, Troung TN, Rai SN, Hancock GC, Lauderdale JG, Joseph T, Truhlar DG (1995) Comput Phys Commun 88:341
32. Truhlar DG (1991) J Comput Chem 12:266
33. Chuang YY, Truhlar DG (2000) J Chem Phys 112:1221
34. Kuchitsu K (1998) In: Structure of free polyatomic molecules basic data, vol 1. Springer, Berlin, pp 156, 102, 104, 138, 111, 141
35. NIST Chemistry WebBook, NIST Standard Reference Database Number 69, June 2005 Release